ARMY RESEARCH LABORATORY

In-Bore Magnetic Field Management

by Alex Zielinski

ARL-TR-1914 March 1999

The findings in this report are not to be construed as an official Department of the Army position unless so designated by other authorized documents.

Citation of manufacturer's or trade names does not constitute an official endorsement or approval of the use thereof.

Destroy this report when it is no longer needed. Do not return it to the originator.

Army Research Laboratory
Aberdeen Proving Ground, MD 21005-5066

ARL-TR-1914 **March 1999**

In-Bore Magnetic Field Management

Alex Zielinski
Weapons and Materials Research Directorate, ARL

Abstract

The turbine/alternator (T/A) in the M734A1 Multi-Option Fuze for Mortar (MOFM) was identified as a component whose performance was altered by exposure to the in-bore magnetic induction produced by the armature in an electromagnetic railgun. Passive shielding techniques were developed to attenuate the exposure field. A model, based on the experimental results, was used to predict shielding effectiveness. Results were verified by subjecting T/As to the exposure field. No statistically significant changes in T/A output were observed for magnetic induction less than *0.06 T*. Significant degradation in performance was observed for magnetic induction greater than *0.1 T*. Active shielding was also demonstrated. This technique was implemented with coil windings mounted in the bore insulators and powered by an external power supply. The in-bore magnetic induction produced by the armature was canceled down-bore of the armature. The technique provides for mitigation of large magnitude exposure fields where otherwise passive shielding may become unwieldy.

REPORT DOCUMENTATION PAGE

Form Approved
OMB No. 0704-0188

1. AGENCY USE ONLY *(Leave blank)*	2. REPORT DATE	3. REPORT TYPE AND DATES COVERED
	March 1999	Final, Oct 97 - Sep 98

4. TITLE AND SUBTITLE

In-Bore Magnetic Field Management

5. FUNDING NUMBERS

1L162622AH80

6. AUTHOR(S)

Alex Zielinski

7. PERFORMING ORGANIZATION NAME(S) AND ADDRESS(ES)

U.S. Army Research Laboratory
ATTN: AMSRL-WM-BC
Aberdeen Proving Ground, MD 21005-5066

8. PERFORMING ORGANIZATION REPORT NUMBER

ARL-TR-1914

9. SPONSORING/MONITORING AGENCY NAMES(S) AND ADDRESS(ES)

10.SPONSORING/MONITORING AGENCY REPORT NUMBER

11. SUPPLEMENTARY NOTES

12a. DISTRIBUTION/AVAILABILITY STATEMENT

Approved for public release; distribution is unlimited.

12b. DISTRIBUTION CODE

13. ABSTRACT ***(Maximum 200 words)***

The turbine/alternator (T/A) in the M734A1 Multi-Option Fuze for Mortar (MOFM) was identified as a component whose performance was altered by exposure to the in-bore magnetic induction produced by the armature in an electromagnetic railgun. Passive shielding techniques were developed to attenuate the exposure field. A model, based on the experimental results, was used to predict shielding effectiveness. Results were verified by subjecting T/As to the exposure field. No statistically significant changes in T/A output were observed for magnetic induction less than *0.06 T*. Significant degradation in performance was observed for magnetic induction greater than *0.1 T*. Active shielding was also demonstrated. This technique was implemented with coil windings mounted in the bore insulators and powered by an external power supply. The in-bore magnetic induction produced by the armature was canceled down-bore of the armature. The technique provides for mitigation of large magnitude exposure fields where otherwise passive shielding may become unwieldy.

14. SUBJECT TERMS

magnetic field, fuze, shielding

15. NUMBER OF PAGES

34

16. PRICE CODE

17. SECURITY CLASSIFICATION OF REPORT	18. SECURITY CLASSIFICATION OF THIS PAGE	19. SECURITY CLASSIFICATION OF ABSTRACT	20. LIMITATION OF ABSTRACT
UNCLASSIFIED	UNCLASSIFIED	UNCLASSIFIED	UL

INTENTIONALLY LEFT BLANK.

Table of Contents

INTENTIONALLY LEFT BLANK.

ACKNOWLEDGMENTS

Dr. Ed Schmidt, the Army's Electric Gun Program Manager, supported this effort. The author would like to extend a generous and sincere appreciation to Mr. George McNally, U.S. Army, Research Development, and Engineering Center (ARDEC) Fuze Division, for providing the turbine/alternators and pre- and post-field exposure test results. Very useful discussions on evaluating magnetic shielding effectiveness for shield materials were provided by Mr. Calvin Le, U.S. Army Research Laboratory, Adelphi Laboratory Center (ARL-ALC). Finally, thanks is extended to Dr. Jubaraj Sahu for providing a timely and thorough technical review of this report.

INTENTIONALLY LEFT BLANK.

List of Figures

INTENTIONALLY LEFT BLANK.

List of Tables

INTENTIONALLY LEFT BLANK

1. INTRODUCTION

The electromagnetic railgun is a launcher capable of accelerating projectiles to hypervelocity. While much attention has focused on performance with kinetic energy penetrators, precision guided munitions (PGMs) are also considered because of their ability to carry electronics and energetic payloads. In principle, PGM launch packages are compatible with railguns. However, there exists the potential for the exposure to the in-bore electric and magnetic fields. It seems reasonable to assume that current technology will be implemented in PGMs launched from railguns. To date, a railgun has not launched a PGM. However, experiments have been conducted where electronic circuit components have been launched from railguns [1, 2, 3]. No deleterious effects on the electronics were noted in these experiments.

A more recent effort focused on the exposure of the Multi-Option Fuze for Mortar (MOFM) circuitry to the in-bore environment [4]. In this investigation, the projectile was restrained in-bore but exposed to field levels consistent with a full-scale hypervelocity weapon. The in-bore environment contained spectra from solid armature and transitioned armature contact operation. While no adverse effects were noted in the function of the radar and microprocessor, minor degradation in the performance of the turbine/alternator (T/A) was noticed. The T/A is used in the MOFM to supply electrical power to the circuitry while the round is in flight. The flow of air is diverted through a port in the nose to the turbine, which is located roughly *40 mm* aft of the nose. The turbine is attached to the alternator on a common shaft. The rotor in the alternator contains permanent magnets to provide the excitation field in the alternator. When the rotor spins, the stator windings produce an output voltage that is used to supply power to the on-board electronics. The exposure to the in-bore field caused the permanent magnets in the T/A to become slightly demagnetized. There was less force retarding the motion of the rotor and, for a given air flow, the rotor was able to spin at a higher velocity. Hence, the T/A produced a higher frequency output. The permanent magnets also provided the excitation field that produced the output voltage. With a lower excitation field, the voltage magnitude decreased.

In the tests reported here, the magnitude of the exposure field was increased by *25%* from previous tests. Conducting materials were then used to reduce the fields with emphasis on increasing the survivability of the component. Moreover, *25* T/As were subjected to the fields. A somewhat statistical representation of the effect of the exposure is generated as a function of the field exposure levels. A picture of the M734A1 fuze body and T/A is shown in Figure 1.

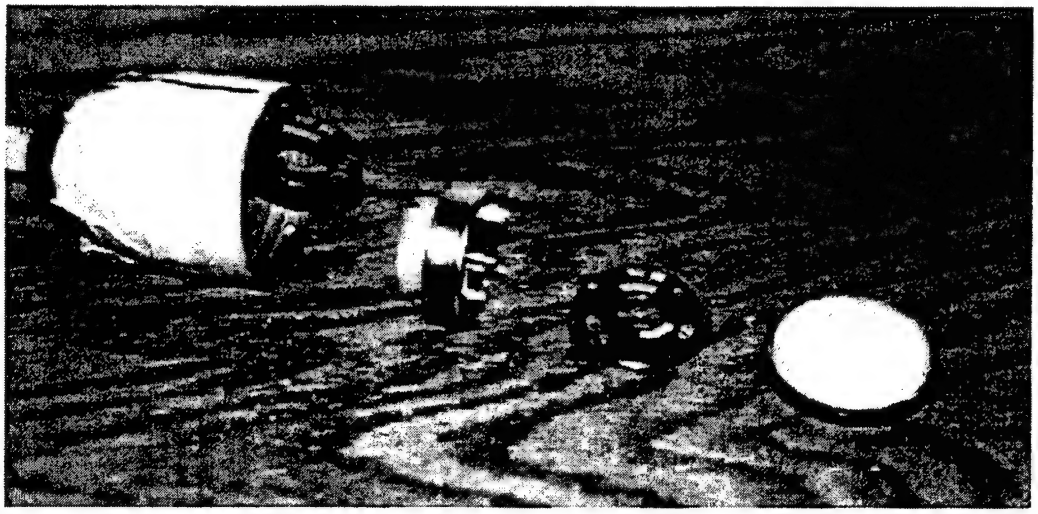

Figure 1. Picture of the M734A1 Fuze. Shown From Left to Right Are the Fuze Body, T/A, Backing Plate, and Fuze Mount.

In addition to attenuating the fields by using conducting materials, magnetic fields can be reduced by supplying a magnetic field that is 180^{o} out of phase with the source field. This technique, called active shielding, is easily accomplished by pulsing a small coil located in the bore with a current that is similar in wave-shape to the current flowing in the armature. An experiment was conducted whereby the active shielding technique was used to reduce the in-bore field.

This report is organized as follows. Section 2 describes the experimental arrangement. Materials are described for attenuating the field. Section 3 presents the results from exposing the T/As. Section 4 describes experimental results for an active shield configuration, and finally, Section 5 contains the summary and conclusions.

2. EXPERIMENT

This section addresses the experiment and tests used to generate and attenuate the in-bore magnetic field. Some success had been achieved using analytical approaches for the attenuation of alternating and static induction fields [5]. However, because of the three-dimensional geometry, transitory nature, and nonlinear behavior of magnetic materials, an experimentally based modeling approach was adopted. The exposure field was *25%* greater than previously generated [4]. Conducting materials were evaluated that would attenuate the exposure field to a level equal to that previously generated and a value *25%* less than that. Once the configurations were selected that could accomplish this task, the T/As were shielded and exposed to these fields.

The T/A was located in the body of the fuze approximately *15 mm* from the base of the fuze body. The experiment was configured so that the in-bore magnetic field was the same that would be generated in a full-scale hypervelocity railgun launching a PGM with electronics located five bore diameters ahead of the armature. In prior measurements, the field was measured at the T/A location to be *0.084 T* at an initial capacitor voltage of *2 kV*. The current flowing in the armature was *233 kA* and rose to peak in *0.45 ms*. In order to generate a *25%* increase in the exposure field, with the T/A located in the same location, a *25%* increase in the initial charge voltage (*2.5 kV*) was required. The resultant magnetic field was *0.105 T*.

The magnetic fields were measured as a function of the axial length of the launcher with a probe that senses the time rate of change in the magnetic induction field (dB/dt). The probe was constructed from seven turns of *24*-gage wire wound on a polyethylene form. The probe had a uniform frequency response to *6 MHz* [4] and was calibrated in a transverse electromagnetic wave cell. The probe was mounted in a polyethylene cylinder (i.e., probe mount) on the centerline of the bore. The cylinder had an outside diameter equal to the diameter of the body of the fuze (*43 mm*). Cylinders of conducting materials, formed from sheet material, were placed on the probe mount and exposed to the in-bore fields. The ratio of the measured field without the shield material to the measured field with the shield material in place is called the magnetic shielding effectiveness (MSE). Typically, the MSE is complex. However, in this report, only the

magnitude of the fields is considered. For magnetic materials, MSE will be a function of the incident induction field since the magnetic permeability is dependent on the field.

The selection of materials was based on availability of materials and prior experience [6]. Materials tested in this investigation included TI-Shield, MμShield, and copper. TI-Shield is a composite material composed of copper, Permalloy 49, and copper. MμShield is a high-permeability magnetic foil, annealed for low shock sensitivity. The maximum length considered was *60 mm* and covered the full length of the fuze body. Additionally, a ring shield configuration was *19 mm* long and was centered over the T/A. Still, another test was conducted where one end of the full shield was enclosed. Also, shield configurations were evaluated where the seams of the shield were taped together and soldered together. The influence of the seams should be minimal since they were aligned in the rail-plane and, therefore, were not coincident with the component of field produced by the armature. The rails, armature, restraint, and shield material (with probe internal to the shield) are shown in Figure 2. A summary of the materials selected and the configurations for use in this experiment are listed in Table 1.

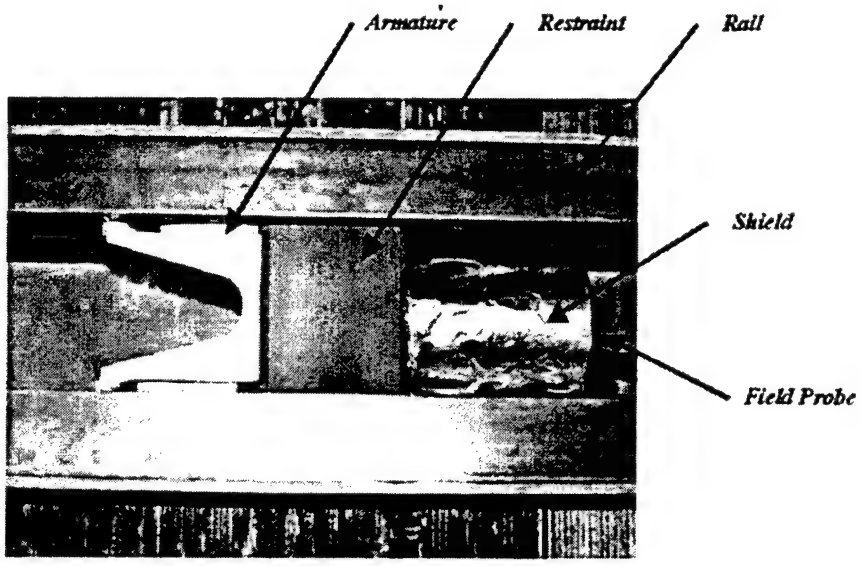

Figure 2. Picture of the Experimental Arrangement.

TABLE 1. SUMMARY OF SHIELDING MATERIALS

- Material thickness = *0.254 mm* (*0.01 in*)
  - Copper: Full length (*70 mm*)
  - MμShield: Full length (*70 mm*), taped
  - TI-Shield: Full length (*70 mm*), taped, soldered
- Material thickness = *0.635 mm* (*0.025 in*)
  - TI-Shield: Full length (*70 mm*), full length with end cap, ring (*19 mm*), soldered, taped

The in-bore magnetic field was measured at two locations: the T/A location, *63 mm* aft of the armature, and *29 mm* further down-bore. These locations are within the axial space of the full-length shield. Initial charge voltages of *1, 2, and 3 kV* were used. These tests provided for six measurements of *dB/dt* that covered a range of incident fields from *0.02 T to 0.14 T.*

Shown in Figure 3 are data for the *0.635-mm* (*0.025 in*) materials. As expected, the MSE decreased as the exposure field increased. Both the soldered and taped cylinders provided roughly the same MSE, although the MSE decreased slightly for the soldered cylinder. The soldered ring configuration had the lowest MSE. Because of the relatively small length-to-diameter ratio, the field was able to extend into the relatively short interior of the cylinder.

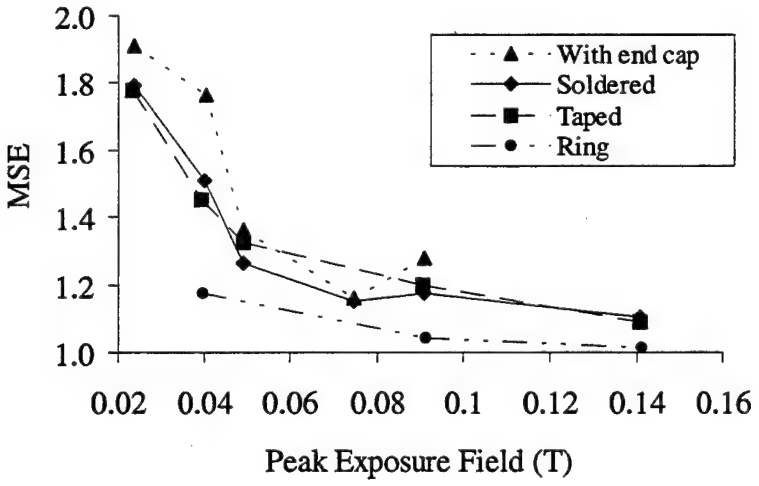

Figure 3. MSE Data for the *0.635 mm* (*0.025 in*) Thick Materials.

This effect is consistent with prior work [5]. The largest MSE was provided by the cylinder configuration with the end closest to the armature closed using *0.635-mm* (*0.025 in*) TI-Shield.

Shown in Figure 4 are data for the *0.254-mm* (*0.01 in*) materials. The MSE decreased for increased exposure field levels, similar to the MSE for the *0.635-mm* (*0.025 in*) data. The smallest MSE was for the copper material. Since the relative permeability for copper is unity, the MSE does not vary significantly as a function of the incident field. The field is excluded from the interior of the shield by the eddy currents that are generated in the relatively good conductor. The variability in the measured data at low exposure fields is due to measurement error. MμShield material provides for a significantly larger MSE for incident fields less than *0.060 T*. The cylinder fabricated from TI-Shield provided the largest MSE. The taped seam did not affect the MSE. Unlike the *0.635 mm* (*0.025 in*) TI-Shield, there was a larger difference between configurations using taped and soldered seams. The *0.254-mm* (*0.01 in*) TI-Shield was not able to adequately dissipate the heat generated during the soldering process.

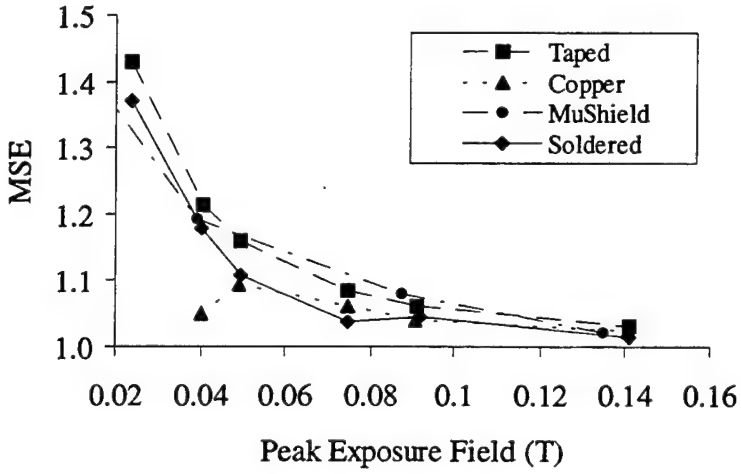

Figure 4. MSE Data for the *0.254 mm* (*0.01 in*) Thick Materials.

The heat from soldering adds carbon to the surface layer of the shield (i.e., carburizing), which results in a lower relative permeability. Both TI-Shield configurations, however, provided for slightly larger MSE than the MμShield material. This is because the TI-Shield is a composite material and the copper provides for the additional shielding when the induction field is large.

The data for the single layer materials shown in Figures 3 and 4 were fit to a function of the form

$$MSE = ZB_o^n + 1, \tag{1}$$

where B_o was the exposure field. The constants for each material, Z and n, were fit using a regression analysis. The fitting constants are listed in Table 2. Full-length shields are used (*70 mm*) unless specified otherwise. The attenuated field can be found from the ratio B_o/MSE.

TABLE 2. FITTING CONSTANTS FOR SHIELD MATERIALS

Material	*n*	*Z*
0.254 mm (0.01 in)		
Copper	-0.7604	0.0065
TI-Shield (taped)	-1.4942	0.0017
TI-Shield (soldered)	-1.8390	0.0004
MμShield (taped)	-1.2401	0.0026
0.635 mm (0.025 in)		
TI-Shield (taped)	-1.1510	0.0106
TI-Shield (soldered)	-1.1851	0.0091
TI-Shield (ring, *19 mm*)	-1.8892	0.0004
TI-Shield (with end cap)	-1.1856	0.0118

The data in Figures 3 and 4 indicate that more than one layer will be needed to attenuate the field to the desired levels. Equation 1 and Table 2 were used to assess the performance of multilayered shield configurations. Shown in Figure 5 is the shield performance for an initial charge voltage of *2 kV* (*0.085 T*). Measured data are provided for the *0.254-mm* (*0.01 in*) TI-Shield material. For comparison, calculations are provided for *0.254-mm* (*0.01 in*) copper and soldered TI-Shield. The data are in good agreement with the calculated MSE up to five layers.

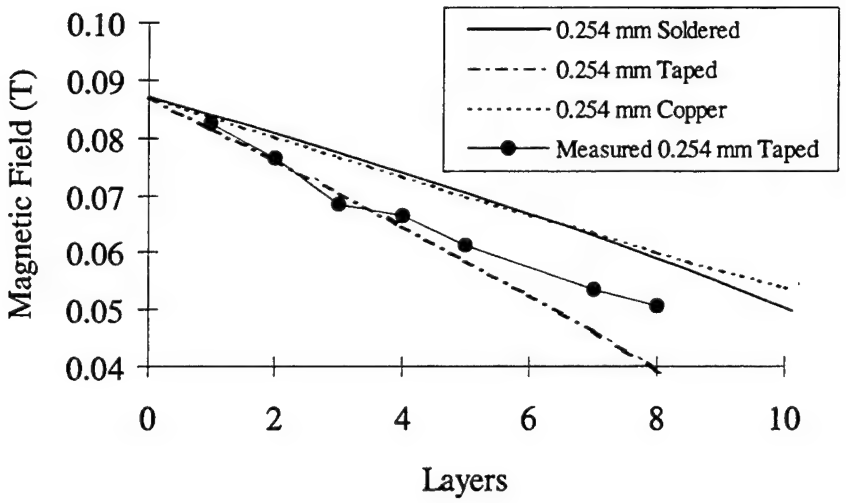

Figure 5. Multilayered MSE for an Initial Charge Voltage of *2 kV* (*0.085 T*).

Beyond five layers, the materials were in close proximity to the rails. It is suspected that currents induced in the outer layer of the shield material are effective at inducing eddy currents in the rails. These induced currents generate induction fields that effectively combine with the armature field and diminish the effectiveness of the shielding at the outer layers. The calculations also indicate the ineffectiveness of the copper and soldered TI-Shield configurations. As noted for the single layer tests, the soldered TI-Shield provided a negligible increase in MSE over the copper material.

Multilayered shielding effectiveness was calculated for the available materials assuming an armature induction field of *0.105 T*. The field on the interior of the shielding configuration at the T/A location is shown in Figure 6. Horizontal lines indicate the desired level of performance. The TI-Shield materials are able to meet the desired level of field exposure. Additionally, there are two vertical lines in the plot. These lines indicate the maximum number of layers in the bore of the railgun based on available space between the outer diameter of the fuze body and the inside surface of the rails.

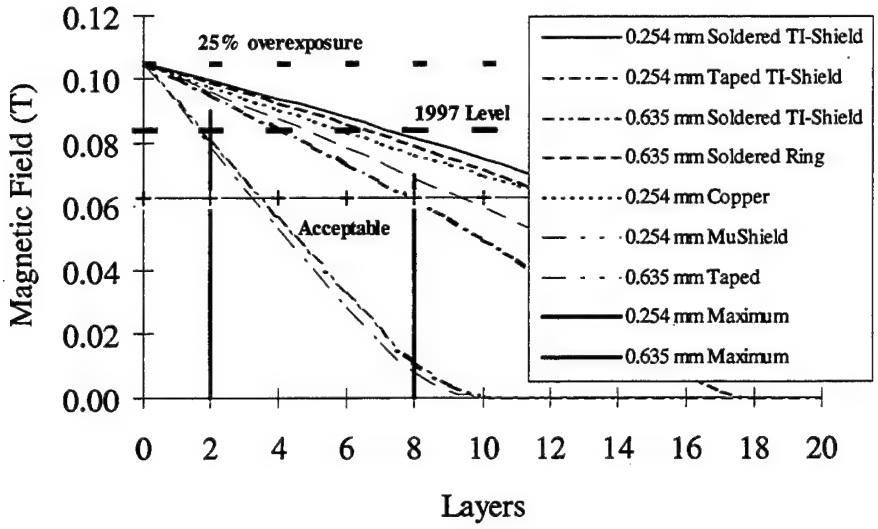

Figure 6. Field at the T/A Location for Multilayered Configurations.

The multilayered MSE of the TI-Shield was evaluated on a per-thickness basis. The MSE was converted to attenuation in *db*. Shown in Figure 7 is the MSE' (*db/mm*) for an exposure field of *0.105 T*.

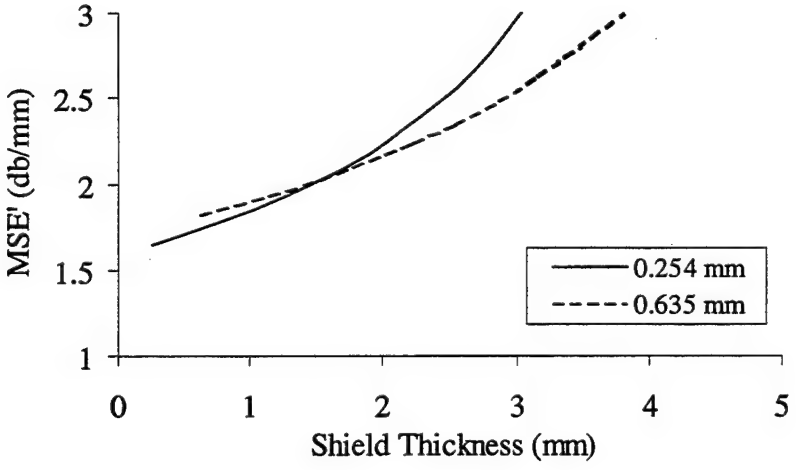

Figure 7. MSE' as a Function of Shield Thickness for an Exposure Field of *0.105 T*.

It can be seen that for an overall thickness less than *1.5 mm* the *0.635 mm* (*0.025 in*) thick material was more effective at attenuating the field. For available space greater than *1.5 mm*, the *0.254 mm* (*0.01 in*) material was more effective at attenuating the field. If, however, the exposure field was increased above *0.105 T*, then the *0.635 mm* (*0.025 in*) thick material was more effective at reducing the field. The attenuation of incident fields greater than approximately *0.1 T* was very difficult to accomplish with a minimal thickness of shield material. Exposure fields less than *0.1 T* are most effectively attenuated by the *0.254 mm* (*0.01 in*) TI-Shield.

Because of the difficulty in handling the *0.635 mm* (*0.025 in*) thick material and its smaller MSE', the *0.254 mm* (*0.01 in*) thick material was selected for shielding the T/As. Four layers and eight layers were selected to reduce the field to the previous exposure level (*0.084 T*) and a further *25%* reduction (*0.060 T*), respectively. In addition to the full-length shield configurations, a ring configuration having eight layers, fabricated from *0.254 mm* (*0.01 in*) TI-Shield, was also selected for testing with the T/As. A photograph of the three shield configurations mounted on the fuze bodies is shown in Figure 8. The exposure field at the T/A location was measured for the selected shield configurations. Shown in Figure 9 is the measured magnetic induction as a function of time. It can be seen that peak exposure levels consistent with the model predictions (see Figure 6) are attained. Although not considered in this report, substantial time delay to reach peak field is observed for increased shield thickness. A fully time-dependent treatment, which is beyond the scope of this effort, is needed to more accurately model the experimental results.

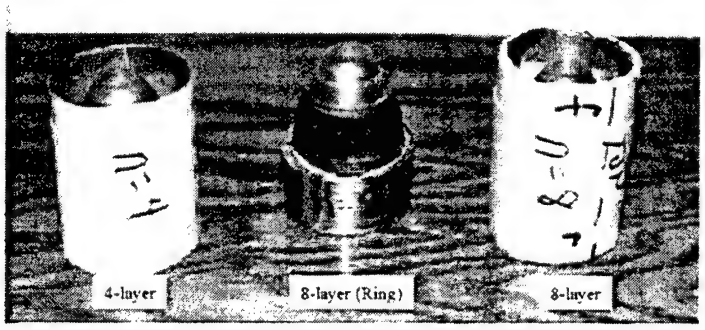

Figure 8. Photograph of Shield Configurations Mounted on the Fuze Bodies.

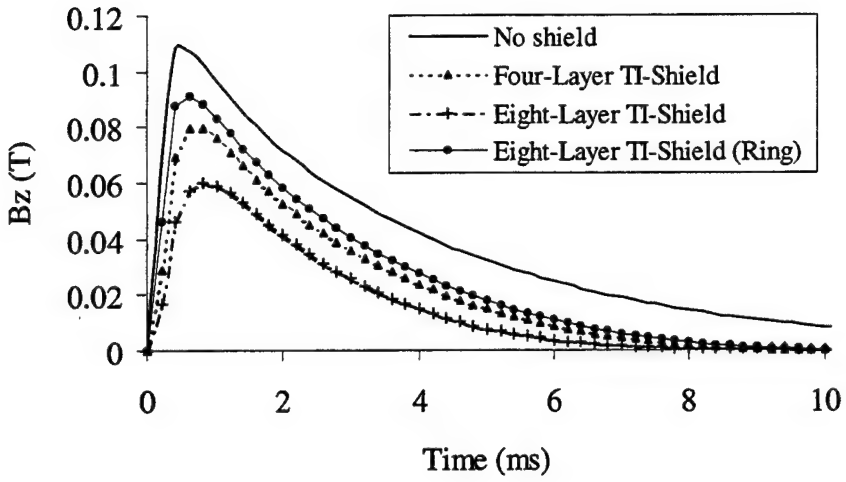

Figure 9. Measured Magnetic Induction as a Function of Time.

3. TEST RESULTS FOR THE T/A

Twenty-five T/As were tested on the effects of the exposure fields. The initial charge voltage was *2.5 kV*, which produced a peak armature current of *280 kA* and a peak exposure field at the T/A location of *0.105 T*. Five units were subjected at each shield configuration. Four T/As were subjected to single-exposure induction fields at initial charge voltages of *1.0, 1.5, 2.0,* and *3.0 kV*. The remaining T/A was not exposed to any in-bore field. All units were tested for voltage and frequency output prior to and after exposure tests.

The data taken on the T/As prior to exposure were used to compute an average output voltage and frequency. The variability was used to determine the standard deviation that normally exists in the T/As. The variability was expressed as a percent change from the average values. The variability in the average output voltage of the T/A is shown in Figure 10. The abscissa is labeled in order of increasing exposure field for the four configurations tested (see Figure 9). The degradation in the output voltage was significant for the exposure with no shielding. The four-layer shield configuration produced an exposure field nearly equivalent to

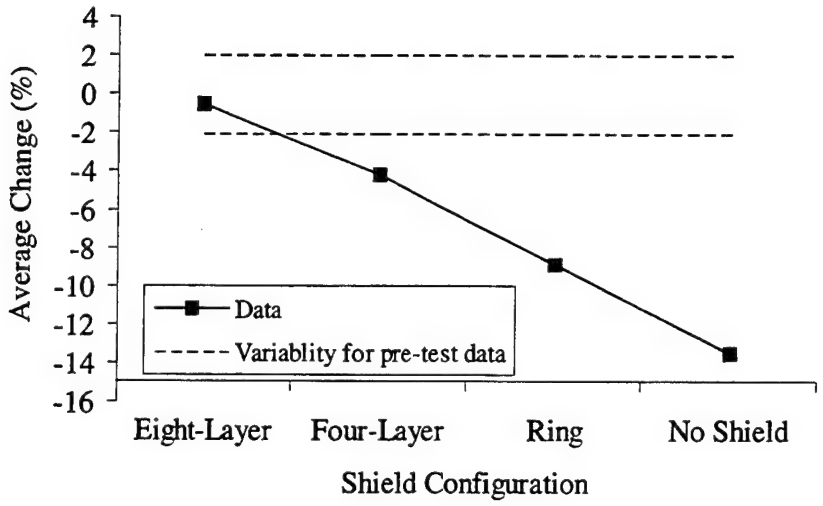

Figure 10. Variability in the Output Voltage for the T/As .

exposure fields from previous tests [4]. In those tests, albeit with limited quantity T/As, some minor change in output voltage was also noted and is consistent with the results presented in Figure 10. The eight-layer shield configuration provided adequate attenuation for the T/A as compared to the variability for the unexposed T/As. Shown in Figure 11 is the variability in output frequency for the four shield configurations.

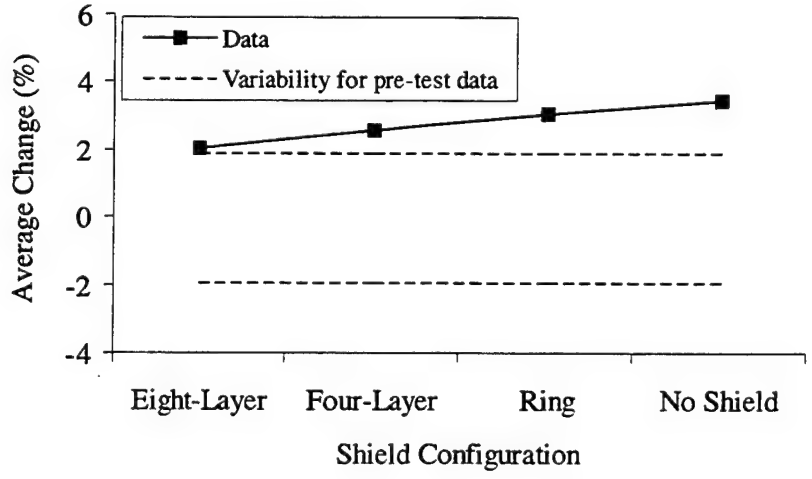

Figure 11. Variability in the Output Frequency for the T/As.

Although not as extreme as the voltage data, statistically, significant differences are seen for the high-exposure field (i.e., no shield). These data are also consistent with prior results [4].

Data were taken for T/A exposure without shield configurations for initial charge voltages from *1 to 3 kV*. The data at *2.5 kV* (*0.105 T*) were taken from the tests for five T/As. Shown in Figure 12 is the change in the output voltage. Although these data were based on the exposure of a single T/A for a single pulse, the change in T/A performance was consistent with the data for multiple T/As (see Figure 10). A similar plot is shown in Figure 13 for the change in the T/A output frequency. This data, and the data presented in Figure 11, showed a slight degradation in the frequency output.

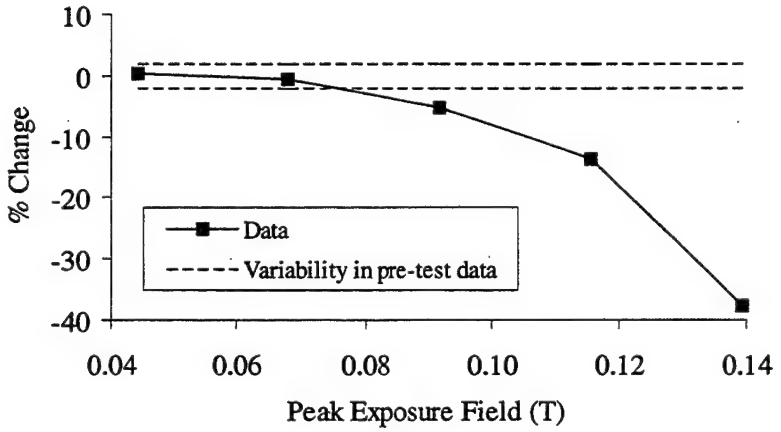

Figure 12. Change in Output Voltage as a Function of Exposure Field (Single Unit Tests).

While the data shown in Figures 10 through 13 indicated the effect of the induction field on T/A performance as well as the effectiveness of managing the field, the shield configuration influences the performance of the radar located in the fuze body. A plot of the antenna gain (i.e., radiated power) of the radar for the eight-layer shield configuration (full length) mounted on the body of the fuze is shown in Figure 14.

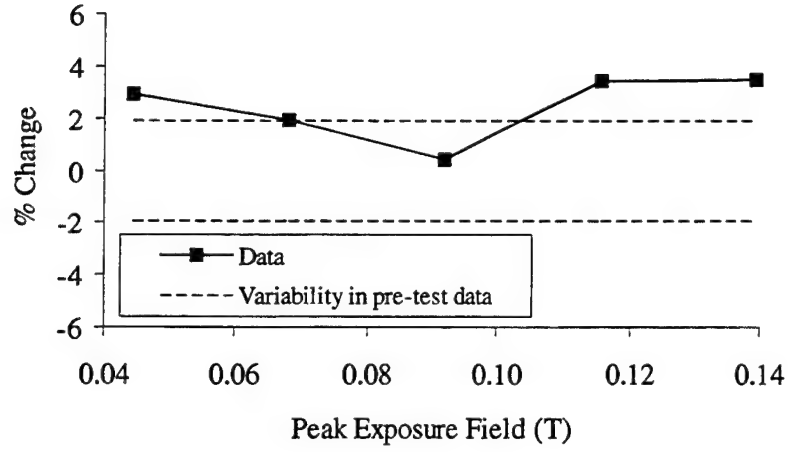

Figure 13. Change in Output Frequency as a Function of Exposure Field (Single Unit Tests).

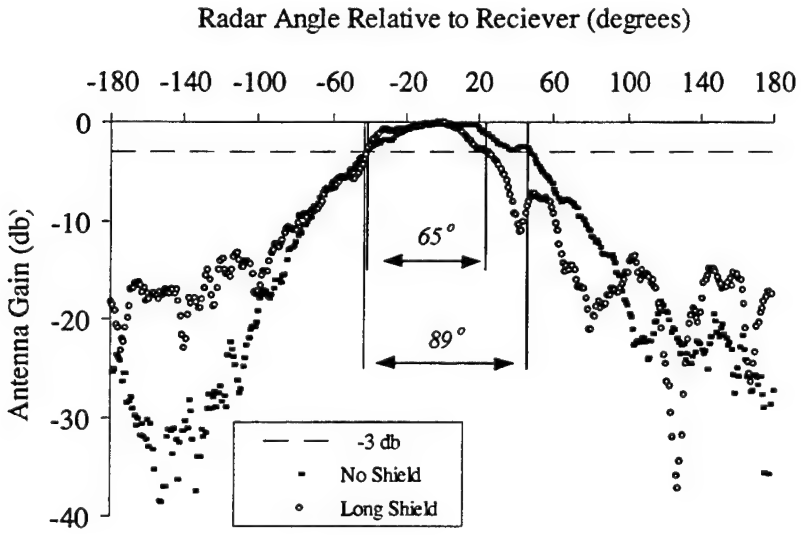

Figure 14. Radar Antenna Gain for No Shield and Eight-Layer Shield Configuration.

The angle of the fuze is defined relative to the receiving antenna. An angle of 0^o corresponds to the nose of the fuze pointed directly at the receiving antenna while 180^o corresponds to the fuze pointed away from the receiving antenna. It can be seen that the beam width, defined by the *–3-db* level, decreased from 89^o to 65^o for the unshielded and shielded configurations, respectively. Although not plotted, less reduction in beam width, and MSE, is

observed for the ring-shield configuration. Effective field management must consider integration of the shield configuration with the performance of other PGM components.

4. ACTIVE SHIELDING

As mentioned in Section 2, the attenuation of magnetic induction fields greater than *0.1 T* becomes untenable. Active shielding can overcome this limitation, provided the added burden of coil windings and electronics can be more easily integrated into the PGM. In this section, measurements and an experiment are presented to illustrate the active shielding concept.

A schematic illustration of the experimental arrangement is shown in Figure 15. The illustration shows the configuration as viewed from the rails. The field generated by the current flowing in the armature generates an exposure field B_{arm}. In this experiment, for convenience, coils were located in the bore insulators and provided for a near uniform field on the centerline of the bore. In practice, the coils are located in the body of the PGM. Again, for convenience, the coils were pulsed with a current from an external power supply.

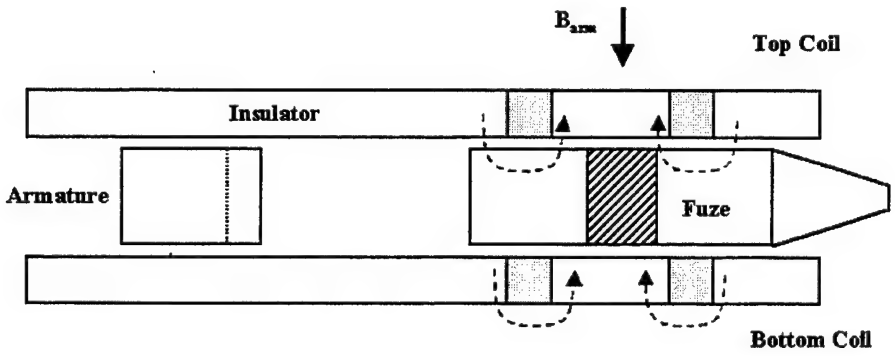

Figure 15. Schematic Illustration of the Active Shield Arrangement.

If implemented in an actual weapon, the magnetic energy associated with the armature could be used to drive a multiturn coil (source) located adjacent to the armature. Additional circuitry is necessary to convert the source voltage, which resembles the time derivative of the armature field, to a source that resembles the armature current.

The armature current rises to peak in *0.45 ms*. Using electrolytic capacitors, which typically have a capacitance of a few *mF* each, requires a coil inductance of a few μH. Selection of an adequate wire gage is essential, since a large circuit resistance will cause the time to reach peak field to occur earlier. The field produced by the armature will not be in-phase with the field produced by the coils, and very little cancellation of the field will occur. Additionally, a minimal number of turns should be used since the coils, when exposed to a *dB/dt*, will generate a voltage that is proportional to the number of turns.

The axial component of the magnetic induction, on the axis of symmetry, due to a current flowing in an *N*-turn circular loop of radius *a*, can be calculated from [7]

$$B_z = \frac{\frac{1}{2}\mu_o a^2 NI}{(a^2 + z^2)^{\frac{3}{2}}}, \tag{2}$$

where μ_o is the permeability of free-space, *I* is the current flowing in the loop, and *z* is the axial distance from the mid-plane of the coil. The magnetic induction for two coils, spaced a distance *d* apart, can be computed using Equation (2) and added at each axial location *z*.

A *50-mm*-diameter coil was constructed in order to measure the axial component of the induction field. Five turns of *14*-gage wire were used. Shown in Figure 16 is the axial component of the induction field as a function of axial location.

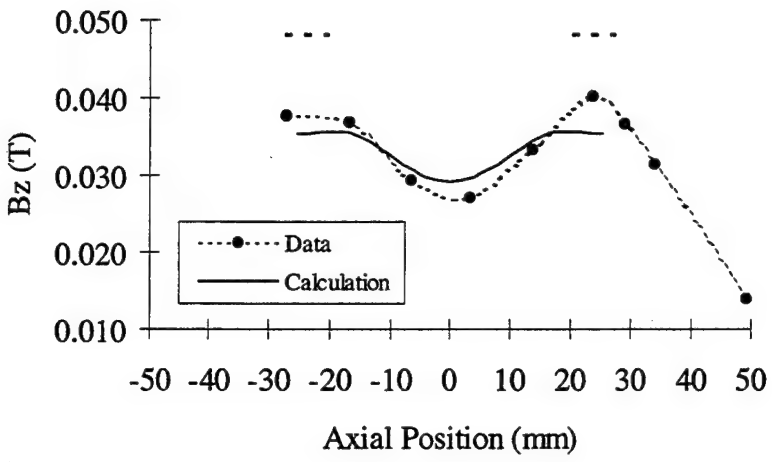

Figure 16. Axial Component of the Magnetic Induction as a Function of Axial Location (*50-mm*-Diameter Coil).

Experiment and theory are shown for a current of *250 A*. The armature field was not present during the test. Also indicated by the two dashed-horizontal lines is the axial length of the coils. As expected, the axial component was fairly constant within the axial extent of the coil windings. As the distance from the coil was increased, the induction field decayed. However, at the distance midway between the two coils, the field was at a minimum of *0.027 T*. Beyond the mid-plane, the field increased due to the influence of the other coil. Finally, beyond the axial extent of the coil, the induction field decayed more rapidly (roughly as $1/z^2$) and was nearly negligible at one coil diameter from the winding. The theory and experiment are in reasonable agreement.

A rectangular coil, shown in Figure 17 and having dimensions of *32 mm* × *76 mm*, was used to generate an in-bore field out of phase with the field produced by a current flowing in the armature.

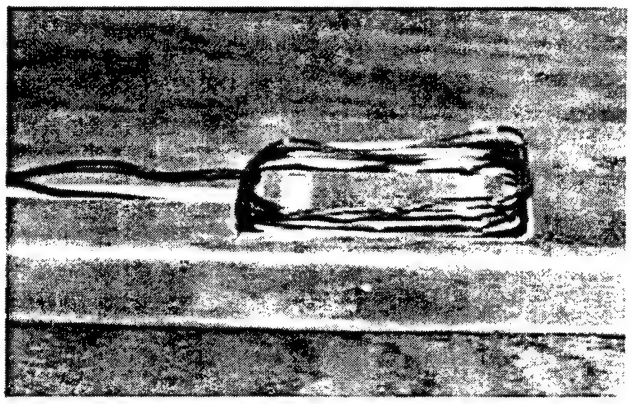

Figure 17. Rectangular Coil Used to Generate the In-Bore Field.

The number of windings was varied and the inductance and resistance were measured with a constant frequency impedance bridge. These results are plotted in Figure 18. The resistance was computed assuming uniform distribution of current in the cross-section of the wire. For *14*-gage copper wire, the resistance per unit length is *8.3 mΩ/m*. The inductance was calculated by equating the coil area (*32 mm* × *76 mm*) to that of an equivalent circular area with radius, *a*. The expression for the inductance is given by [8],

$$L = \frac{\mu_o N^2 \pi a^2 K}{\ell}, \tag{3}$$

where ℓ is the axial length of the coil and K is a function of the ratio a/ℓ and can be determined by

$$K = 0.61(a/\ell)^{-0.7}. \tag{4}$$

Calculated and measured results for the inductance were in good agreement and to a lesser degree for the resistance. Measurements of the resistance are more sensitive to the electrical connections to the impedance-bridge than for the inductance. This error is consistent with the data in Figure 18.

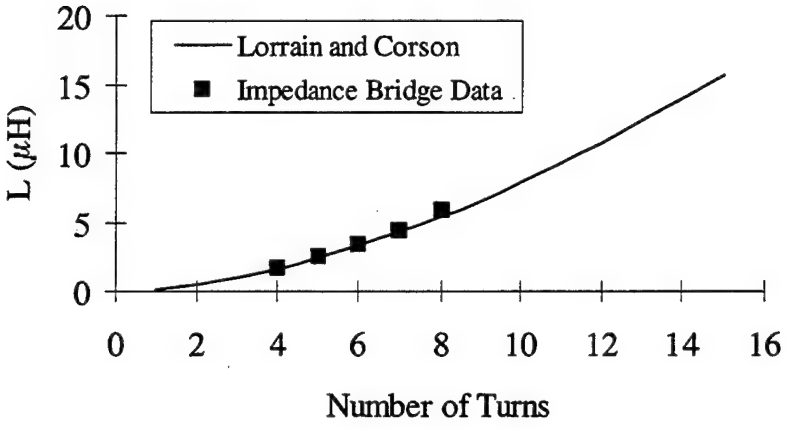

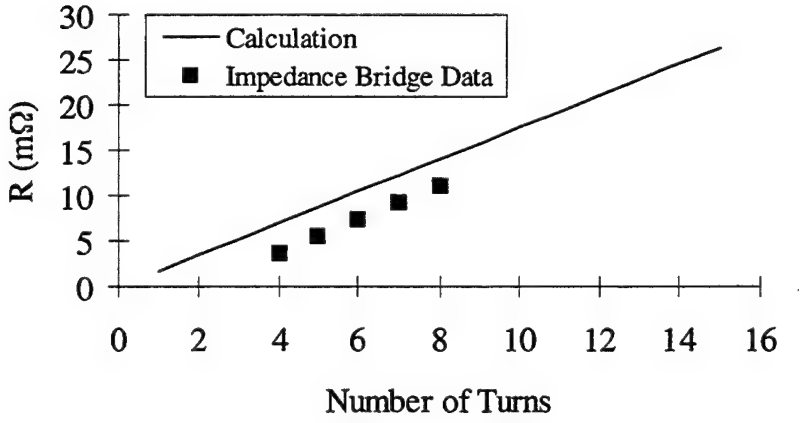

Figure 18. Inductance (Top) and Resistance (Bottom) for a Single Rectangular Coil as a Function of the Number of Turns.

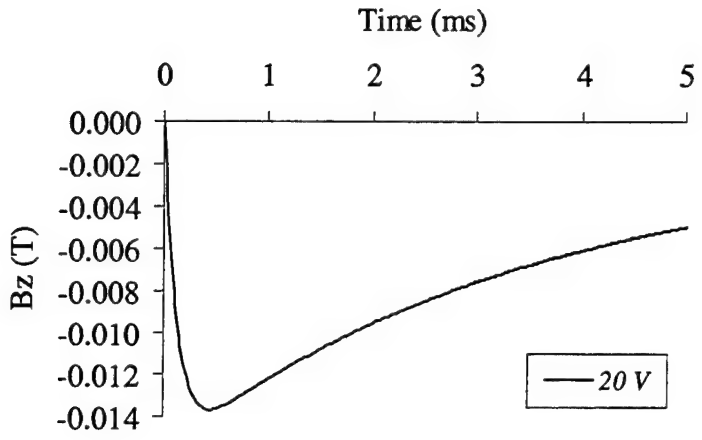

Figure 19. Measured In-Bore Field as a Function of Time for the Rectangular Coil.

Based on the maximum available electrolytic capacitors (*28 mF*), an eight-turn winding was selected for the top and bottom coil. A plot of the measured in-bore field as a function of time is shown in Figure 19 for no current flowing in the armature. With *20 V* on the electrolytic capacitors, the coil produced a peak field of *-0.014 T* at *0.45 ms*.

The results for *107 kA* flowing in the armature are shown in Figure 20. For *50 V* on the capacitors, a current of *296 A* is conducted by the coils and the field produced by the armature is nearly cancelled. The energy stored in the capacitors was *35 J*. However, using the measured inductance of *15.6 μH* gave a stored magnetic energy of *0.7 J*. Not unexpected, the resistive losses for this nonoptimized circuit were rather substantial. If a more realistic efficiency were attained (*20%*), an initial voltage of *15 V* could be used to cancel the armature field. The magnetic field for the in-bore coil pair calculated from Equation (2) is *-0.044 T*. This value is in good agreement with the field measured at *20 V* linearly scaled to the *50-V* test data (*-0.035 T*). The field measured at the T/A location with *107 kA* flowing in the armature is *0.04 T*. It is reasonable that the field generated by the armature was canceled by the field produced by the in-bore coil at an initial charge voltage of *50 V*. The minor negative portion of the measured field for times less than *0.25 ms* was due to the slightly different rate of rise for the field produced by the in-bore coils relative to the armature field.

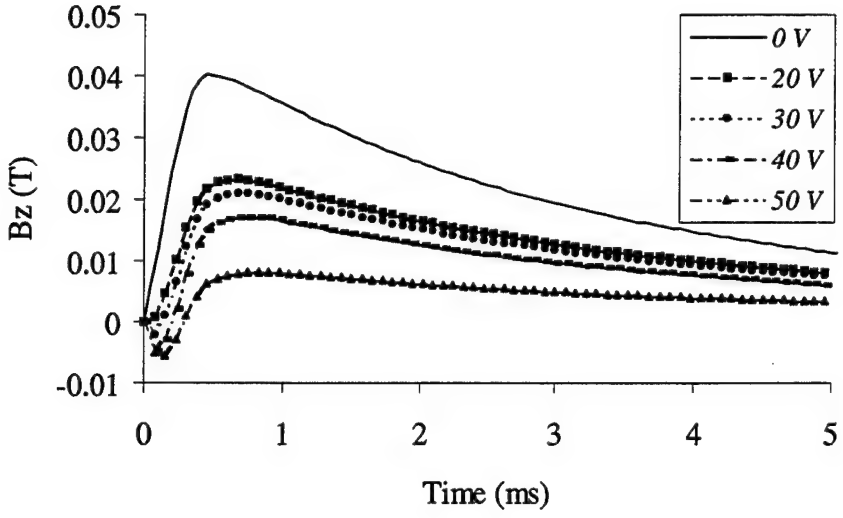

Figure 20. Exposure Field as a Function of Time for the Active Shield Configuration.

With less than *50 V* on the on the electrolytic capacitors, the coils produced proportionately less field. Consequently, a small portion of the in-bore field was cancelled.

5. SUMMARY AND CONCLUSIONS

In-bore exposure forward of the armature, due to the armature induction field, can be reduced to manageable levels. Small, short shields (length-to-diameter ratio less than one) were not as effective as full-length shields with one (or both) ends enclosed. Perhaps the most effective technique for reducing the field on a component is simply to increase the distance between the source field and the component.

Passive shielding utilized conducting materials to attenuate the exposure field. Magnetic materials, whose relative permeability was greater than one, were also used. The test results for the MSE indicated that for exposure fields greater than *0.060 T* the magnetic material saturated. The material no longer provided substantial attenuation of the field. Nonmagnetic materials, whose relative permeability is equal to one, provided a constant attenuation regardless of the

exposure field. For the exposure field considered in this report (*0.105 T*), a composite structure (TI-Shield) provided the optimum shielding. Combinations of materials other than those used in the TI-Shield are possible. However, further optimization was beyond the scope of this effort.

The MSE was proportional to the material thickness. However, the thick materials were difficult to form and join at the seams. Fortunately, the shields were oriented in the bore of the railgun such that the MSE was insensitive to the location of the seams. Soldering should be avoided, especially for thin materials, as the heat from soldering carburized the material, decreased the relative permeability, and reduced the MSE. Efficient use of available space for field attenuation required a large MSE per shielding thickness (MSE'). Since the MSE for magnetic materials was dependent on the induction field, it was not surprising that MSE' was also dependent on the induction field. Generally, for exposure fields less than *0.1 T*, thin TI-Shield (*0.01 in*) provided larger MSE'. Above *0.1 T*, thicker TI-Shield material was more efficient in attenuating the in-bore induction field.

Tests were conducted on the M734A1 MOFM T/A. Passive shielding techniques were incorporated with the fuze body and attenuated the exposure field. The change in T/A performance was determined by examining pre- and post-exposure tests on the T/A voltage and frequency output. Significant degradation in the output voltage was observed for fields greater than *0.1 T*. Minor degradation was observed for *0.08 T* and is consistent with prior experimental results. No statistically significant change was observed for field exposure less than *0.06 T*. Similar results, although to a lesser extent, were observed for the frequency output of the T/A. The peak exposure field was presumed to demagnetize the magnets in the rotor of the T/A.

Active shielding can be efficiently implemented for field attenuation where the exposure field is much greater than *0.1 T* and available space is limited. An experiment was conducted using windings located in the bore of the railgun and an external power supply. Only *0.7 J* of peak magnetic energy was required to cancel the field generated by the armature. Further work is needed to generate the coil field from the inherent magnetic energy of the armature.

Large power and energy are necessary to operate hypervelocity electromagnetic railguns. These electrical quantities provide an in-bore environment that is rich in electric and magnetic fields. Despite potential deleterious effects on sensitive PGM components, no disastrous consequences were observed. Furthermore, one component was identified that developed anomalies in its performance and, using passive shielding, was successfully ameliorated.

INTENTIONALLY LEFT BLANK

REFERENCES

1. Heyse, M., and K. Jamison. "In-Bore Measurements of Lateral Acceleration of a Solid Armature Driven Electromagnetic Launcher Projectile." Wright Laboratory, Armament Directorate, Eglin Air Force Base, FL, WL-TR-7017, March 1996.

2. Heyse, M., J. Batteh, J. Scanlon, and L. Thornhill. "In-Bore Measurements of Magnetic Field in Front of the Armature and Soft Catch of Electromagnetic Launcher Projectiles." Wright Laboratory, Armament Directorate, Eglin Air Force Base, FL, WL-TR-7020, March 1996.

3. Schroder, K. A., R. J. Allen, J. V. Parker, and P. T. Snowden. "In-Bore Measurements Using an Optical Data Link." *IEEE Transactions on Magnetics*, vol. 35, no. 1, January 1999.

4. Zielinski, A. E., C. Le, and J. A. Bennett. "In-Bore Electric and Magnetic Field Environment." *IEEE Transactions on Magnetics*, vol. 35, no. 1, January 1999.

5. Mager, A. "Magnetic Shields." *IEEE Transactions on Magnetics,* vol. Mag-6, no.1, March 1970.

6. Le, C. D., and A. E. Zielinski. "Preliminary Findings on Magnetic Shielding Effectiveness for Electromagnetic (EM) Railgun Applications." Presented and published in the *Proceedings of the 6th European Electromagnetic Launcher Symposium (EEMLS)*, May 1997.

7. Smythe, W. R. *Static and Dynamic Electricity.* 2nd Edition, NY, McGraw-Hill Book Company, Inc., 1950.

8. Corson, D. R., and P. Lorrain. *Introduction to Electromagnetic Fields and Waves.* 2nd Edition, NY, W. H. Freeman publisher, 1970.

INTENTIONALLY LEFT BLANK

NO. OF COPIES ORGANIZATION

2 DEFENSE TECHNICAL INFORMATION CENTER
DTIC DDA
8725 JOHN J KINGMAN RD
STE 0944
FT BELVOIR VA 22060-6218

1 HQDA
DAMO FDQ
DENNIS SCHMIDT
400 ARMY PENTAGON
WASHINGTON DC 20310-0460

1 OSD
OUSD(A&T)/ODDDR&E(R)
R J TREW
THE PENTAGON
WASHINGTON DC 20301-7100

1 DPTY CG FOR RDE
US ARMY MATERIEL CMD
AMCRD
MG CALDWELL
5001 EISENHOWER AVE
ALEXANDRIA VA 22333-0001

1 INST FOR ADVNCD TCHNLGY
THE UNIV OF TEXAS AT AUSTIN
PO BOX 20797
AUSTIN TX 78720-2797

1 DARPA
B KASPAR
3701 N FAIRFAX DR
ARLINGTON VA 22203-1714

1 NAVAL SURFACE WARFARE CTR
CODE B07 J PENNELLA
17320 DAHLGREN RD
BLDG 1470 RM 1101
DAHLGREN VA 22448-5100

1 US MILITARY ACADEMY
MATH SCI CTR OF EXCELLENCE
DEPT OF MATHEMATICAL SCI
MAJ M D PHILLIPS
THAYER HALL
WEST POINT NY 10996-1786

NO. OF COPIES ORGANIZATION

1 DIRECTOR
US ARMY RESEARCH LAB
AMSRL D
R W WHALIN
2800 POWDER MILL RD
ADELPHI MD 20783-1145

1 DIRECTOR
US ARMY RESEARCH LAB
AMSRL DD
J J ROCHIO
2800 POWDER MILL RD
ADELPHI MD 20783-1145

1 DIRECTOR
US ARMY RESEARCH LAB
AMSRL CS AS (RECORDS MGMT)
2800 POWDER MILL RD
ADELPHI MD 20783-1145

3 DIRECTOR
US ARMY RESEARCH LAB
AMSRL CI LL
2800 POWDER MILL RD
ADELPHI MD 20783-1145

ABERDEEN PROVING GROUND

4 DIR USARL
AMSRL CI LP (305)

NO. OF COPIES	ORGANIZATION
1	DIR FOR THE DIRECTORATE OF FORCE DEVELOPMENT US ARMY ARMOR CTR COL E BRYLA FT KNOX KY 40121-5000
1	USAMC AMC DCG T C KITCHENS 5001 EISENHOWER BLVD ALEXANDRIA VA 22333-0001
2	USARL C LE G MCNALLY AMSRL 2800 POWDER MILL RD ADELPHI MD 20783-1145
1	DPTY ASST SEC FOR RD AND A R CHAIT THE PENTAGON RM 3E480 WASHINGTON DC 20310-0103
1	OFC OF THE DIR DEFENSE RSRCH AND ENGRG C KITCHENS 3080 DEFENSE PENTAGON WASHINGTON DC 20301-3080
1	USAMC AMSMI RD DR MCCORKLE REDSTONE ARSENAL AL 35898-5240
2	US ARMY TACOM TARDEC J CHAPIN M TOURNER AMSTA TR D MS 207 WARREN MI 48397-5000
1	US ARMY TACOM ARDEC J BENNETT FSAE GCSS TMA BLDG 354 PICATINNY ARSENAL NJ 07806-5000

NO. OF COPIES	ORGANIZATION
3	INST FOR ADVANCED TECH UNIV OF TEXAS AT AUSTIN P SULLIVAN F STEPHANI 4030 2 WEST BRAKER LN AUSTIN TX 78759-5329
4	UNIV OF TEXAS AT AUSTIN CTR FOR ELECT A WALLS J KITZMILLER S PRATAP PRC MAIL CODE R7000 AUSTIN TX 78712
1	LOCKHEED MARTIN VOUGHT R TAYLOR PO BOX 650003 MS WT 21 DALLAS TX 75265-0003
1	INST FOR DEFENSE ANALYSIS I KOHLBERG 1801 N BEAUREGARD ST ALEXANDRIA VA 22311
1	UNIV AT BUFFALO SUNY AB J SARJEANT PO BOX 601900 BUFFALO NY 14260-1900
2	UDLP B GOODELL R JOHNSON MS M170 4800 EAST RIVER RD MINNEAPOLIS MN 55421-1498
1	UNIV OF TEXAS AT AUSTIN M DRIGA ENS 434 DEPT OF ECE MAIL CODE 60803 AUSTIN TX 78712

NO. OF COPIES	ORGANIZATION
1	SAIC G CHRYSSOMALLIS 3800 WEST 80TH ST SUITE 1090 BLOOMINGTON MN
1	SAIC J BATTEH 1225 JOHNSON FERRY RD SUITE 100 MARIETTA GA 30068
1	SAIC K A JAMISON 1247 B N EGLIN PKWY SHALIMAR FL 32579
2	IAP RESEARCH INC D BAUER J BARBER 2763 CULVER AVE DAYTON OH 45429-3723
3	MAXWELL TECHNOLOGIES J KEZERIAN P REIDY T WOLFE 9244 BALBOA AVE SAN DIEGO CA 92123
1	NORTH CAROLINA STATE UNIV M BOURHAM DEPT OF NUCLEAR ENGR BOX 7909 RALEIGH NC 27695-7909
1	MAXWELL PHYSICS INTRNTL C GILMAN 2700 MERCED STREET PO BOX 5010 SAN LEANDRO CA 94577-0599

NO. OF COPIES	ORGANIZATION
	ABERDEEN PROVING GROUND
23	DIR USARL AMSRL WM I MAY L JOHNSON AMSRL WM B A HORST E SCHMIDT AMSRL WM TE J POWELL AMSRL WM BE G WREN AMSRL WM BD B FORCH AMSRL WM BA W DAMICO AMSRL WM BC P PLOSTINS D LYON J GARNER V OSKAY M BUNDY J SAHU P WEINACHT H EDGE B GUIDOS A ZIELINSKI D WEBB K SOENCKSEN S WILKERSON T ERLINE J NEWILL

INTENTIONALLY LEFT BLANK.

USER EVALUATION SHEET/CHANGE OF ADDRESS

This Laboratory undertakes a continuing effort to improve the quality of the reports it publishes. Your comments/answers to the items/questions below will aid us in our efforts.

1. ARL Report Number/Author ARL-TR-1914 (Zielinski) Date of Report March 1999

2. Date Report Received _____

3. Does this report satisfy a need? (Comment on purpose, related project, or other area of interest for which the report will be used.) _____

4. Specifically, how is the report being used? (Information source, design data, procedure, source of ideas, etc.) _____

5. Has the information in this report led to any quantitative savings as far as man-hours or dollars saved, operating costs avoided, or efficiencies achieved, etc? If so, please elaborate. _____

6. General Comments. What do you think should be changed to improve future reports? (Indicate changes to organization, technical content, format, etc.) _____

CURRENT ADDRESS

Organization

Name E-mail Name

Street or P.O. Box No.

City, State, Zip Code

7. If indicating a Change of Address or Address Correction, please provide the Current or Correct address above and the Old or Incorrect address below.

OLD ADDRESS

Organization

Name

Street or P.O. Box No.

City, State, Zip Code

(Remove this sheet, fold as indicated, tape closed, and mail.)

(DO NOT STAPLE)